

Intramolecular vibrational redistribution in aromatic molecules. I. Eigenstate resolved CH stretch first overtone spectra of benzene

A. Callegari,^{a)} U. Merker,^{b)} P. Engels,^{b),c)} H. K. Srivastava, K. K. Lehmann, and G. Scoles^{d)}

Department of Chemistry, Princeton University, Princeton, New Jersey 08544

(Received 17 December 1999; accepted 5 September 2000)

We have used infrared–infrared double resonance spectroscopy to record a rovibrational eigenstate resolved spectrum of benzene in the region of the CH stretch first overtone. This experiment is the first of a series aimed at investigating intramolecular vibrational energy redistribution (IVR) in aromatic molecules. The experiment has been carried out in a supersonic molecular beam apparatus using bolometric detection. A tunable resonant cavity was used to enhance the on-beam intensity of the 1.5 μm color center laser used to pump the overtone, and a fixed frequency [$R(30)$] $^{13}\text{CO}_2$ laser was used to saturate the coinciding $\nu_{18}^r Q(2)$ transition of benzene. After assigning the measured lines of the highly IVR fractionated spectrum to their respective rotational quantum number J , analysis of the data reveals that the dynamics occurs on several distinct time scales and is dominated by anharmonic coupling with little contribution from Coriolis coupling. After the fast (~ 100 fs) redistribution of the energy among the previously observed “early time resonances” [R. H. Page, Y. R. Shen, and Y. T. Lee, *J. Chem. Phys.* **88**, 4621 (1988) and **88**, 5362 (1988)], a slower redistribution (10–20 ps) takes place, which ultimately involves most of the symmetry allowed vibrational states in the energy shell. Level spacing statistics reveal that IVR produces a highly mixed, but nonstatistical, distribution of vibrational excitation, even at infinite time. We propose that this nonintuitive phenomenon may commonly occur in large molecules when the bright state energy is localized in a high-frequency mode. © 2000 American Institute of Physics. [S0021-9606(00)00345-7]

I. INTRODUCTION

A. Background

The issue and the very existence of intramolecular vibrational energy redistribution (IVR) was raised in Slater's pioneering dynamical theory of unimolecular reaction rates¹ and the statistical theories of Rice and Marcus^{2,3} and Rosenstock *et al.*,⁴ from which modern theories evolved.^{5,6} In statistical theories, IVR is assumed to be rapid and complete, while in Slater's theory, in which the vibrational modes are assumed to be perfectly harmonic and noninteracting, the reaction proceeds only when a particular superposition of these modes causes the reaction coordinate to reach the top of the reaction barrier. Recently, however, it has become evident that both the assumption of no randomization and that of total randomization are too strong, and that real molecules are better described by an intermediate picture that is closer to one or the other extreme depending on the molecular size, structure, energy, and on the time scale considered.

Two different reasons may prevent complete energy ran-

domization: either an IVR rate that is slow compared to the unimolecular reaction rate, or intrinsically nonergodic dynamics. In the first case the molecular motion simply “does not have the time” to explore all of the available phase space before the reaction occurs. In the second case, instead, the motion is constrained to a subset of the available phase space and complete energy randomization cannot occur, even in an infinite amount of time. Note that, because of the necessary presence of quantum interference, only about one-third of the *a priori* available phase space can be accessed, even with the strongest mixing.⁷ We shall therefore refer to this limit as that of complete (in the quantum sense) energy randomization.

That IVR rates can be slow, even for relatively large molecules (>10 atoms) at energies as high as 6000 cm^{-1} has been observed before. The study of slow IVR (100 ps and longer) was pioneered by Perry and co-workers, with their study of the CH stretching fundamentals of butyne.^{8,9} Quack and co-workers^{10–12} have found that the lifetime of the acetylenic CH stretch fundamental and overtone in various substituted acetylenes could be longer than 10 ps. Later, Lehmann, Scoles and co-workers^{13–16} have studied the IVR of the acetylenic CH stretch in a similar series of substituted acetylenes and found lifetimes as long as several ns. Furthermore, the measured lifetimes appear to be uncorrelated with the magnitude of the total density of states. This phenomenon can be explained^{11,14,17} as due to a lack of low-order couplings, which produces bottlenecks that prevent the fast re-

^{a)}Current address: Laboratoire de Chimie Physique Moléculaire (LCPM), École Polytechnique Fédérale de Lausanne, CH-1015 Lausanne, Switzerland.

^{b)}On leave from the University of Bonn, Institut für Angewandte Physik, Wegelerstr. 8, 53115 Bonn, Germany.

^{c)}Current address: Institut für Quantenoptik, Universität Hannover, Welfengarten 1, 30167 Hannover, Germany.

^{d)}Author to whom correspondence should be addressed. Electronic mail: gscoles@princeton.edu

distribution of energy from the initially excited state.

The issue of ergodic versus nonergodic energy redistribution is somewhat more controversial. Bixon and Jortner¹⁸ have given a set of sufficiency criteria for the existence of irreversible energy redistribution in isolated molecules, requiring strong, uniform coupling matrix elements between the initially prepared state and all other vibrational states, where strong means much larger than the average spacing of vibrational states. The requirement of uniform couplings has been relaxed by Kay^{19,20} to the more likely assumption that the couplings be strong, but allowing them to be statistically independent. Similar assumptions, although applied to quite a different multibody system, lead to the well-known Gaussian Orthogonal Ensemble model proposed by Dyson,²¹ which has worked exceedingly well in explaining the statistical properties of the energy levels of atomic nuclei and has since become the reference model in the study of ergodic dynamics. Small molecules, with a sufficiently low density of states, may not satisfy the strong coupling requirement and hence exhibit nonergodic dynamics. There is, however, some evidence that nonergodic IVR dynamics is possible, even for relatively large molecules (see, e.g., Refs. 22–26). For recent reviews on IVR, see Refs. 11, 23, and 27–29.

B. Current issues

When are the requirements for ergodic dynamics^{19–21} fulfilled (if at all) in a molecule? The aforementioned successes of statistical theories (e.g., RRKM) in predicting the rates of unimolecular reactions, and of random matrix theory³⁰ (e.g., the Gaussian Orthogonal Ensemble model) in predicting the energy spectrum of several different many-body systems, would suggest that most molecules should exhibit ergodic energy redistribution, but a clear answer to the question has yet to be found. It was suggested by Freed and Nitzan,^{31,32} that “perhaps it is the statistical character of the initial state which is responsible for the success of the statistical theories.” As for random matrix theory, its successful description of atomic nuclei may well be related to the peculiar nature of these highly confined and strongly interacting multiparticle systems. It is not obvious to what extent a similar description would be appropriate for modeling molecular dynamics.

In light of the findings discussed in the previous section, it appears that neither the *fast* nor the *democratic* character of the IVR process required by statistical theories should be taken for granted, even in large molecules.

Ideally, one would like to be able to reliably predict the rate and extent of IVR for a given molecule and a given method of excitation, starting from a small number of molecular parameters. Recent theoretical models have been able (starting from semiempirical potential energy surfaces) to successfully reproduce the experimentally observed data in molecules as large as benzene^{33–47} and (CH₃)₃CCCH¹⁷ with densities of states in some cases in excess of 10⁷/cm⁻¹. To what extent is the knowledge gained about these specific molecules transferable to “similar” molecules, and how can the similarity be quantified? To what extent can the observed dynamics be explained by means of some “universal law”

and how much of it instead depends on the fine details of the potential energy surface and of the initially prepared states?

At the two extremes we find the following: on one side the case of total predictability, where some sort of “group behavior” (see, e.g., Refs. 11,48) can be defined and transferred from one molecule to another (analogous to the concept of group frequencies in infrared spectroscopy). On the other side we have total unpredictability, where the dynamics of every individual molecule and initial excitation has to be worked out from first principles with the great expense of computational effort.

A sensible approach is to study a series of molecules large enough (number of degrees of freedom and density of coupled states) to be considered typical, but at the same time with a simple enough structure that allows for accurate modeling. Benzene (C₆H₆), pyrrole (C₄NH₅), and triazine (C₃N₃H₃), the aromatic molecules chosen for this purpose, satisfy all the requirements as “benchmark systems.” They have a reasonably large number of atoms (≈ 10) but a relatively rigid structure that removes the problem of dealing with strongly anharmonic low-frequency motions (e.g., internal rotor torsional modes) that plague other potentially interesting candidates. Hopefully this will make it possible to calculate the most relevant couplings from semiempirical and *ab initio* potential energy surfaces, with sufficient accuracy to make these molecules “textbook models” for the study of vibrational redistribution in a system of coupled oscillators. It is not by chance that one of these molecules (benzene) has become the focus of possibly the largest number of experiments in the history of IVR, as well as a benchmark system for most theoretical models. The first paper of this series will be dedicated to the study of benzene, while the results relating to the other two molecules will be presented later.

C. Previous work on benzene

Numerous theoretical and experimental papers have investigated benzene fundamental^{49–54} and overtone vibrations^{33–47,55–65} and potential energy surface.^{66,67} The observed fundamental frequencies are reported in Table I along with the two commonly used Wilson’s and Herzberg’s naming conventions. Note that throughout the paper we will be consistently using Wilson’s mode numbering.

Since the pioneering work of Berry and co-workers,^{55,57} benzene overtones have become one of the most important model systems for the study of IVR. The early experimental work⁵⁷ investigated the CH stretching fundamental and overtone bands up to $\nu = 9$, but because of extensive inhomogeneous contributions to the measured spectra, their interpretation remained ambiguous. Theoretical modeling by Sibert *et al.*⁴⁰ indicated that the overall spectral width of the visible bands reflects rapid IVR via Fermi resonances between the C–H stretching local modes and the C–H bend normal modes. However, dynamics on a time scale longer than ~ 100 fs could not be inferred from the experimental results due to the rotational and hot band congestion present in these room temperature spectra.

More recent experimental work on the overtone spectrum has exploited free jet cooling of the molecules, which

TABLE I. The observed gas-phase fundamental frequencies of benzene, from Refs. 51 and 67 and references therein. Wilson's mode numbering convention is used throughout this paper.

Sym	Wilson no.	Herzberg no.	$\tilde{\nu}/\text{cm}^{-1}$
a_{1g}	ν_2	ν_1	3073.942
	ν_1	ν_2	993.071
a_{2g}	ν_3	ν_3	1350
b_{1u}	ν_{13}	ν_5	3057
	ν_{12}	ν_6	1010
b_{2u}	ν_{14}	ν_9	1309.4
	ν_{15}	ν_{10}	1149.7
	ν_7	ν_{15}	3056.7
e_{2g}	ν_8	ν_{16}	1600.9764
	ν_9	ν_{17}	1177.776
	ν_6	ν_{18}	608.13
	ν_{20}	ν_{12}	3064.3674
e_{1u}	ν_{19}	ν_{13}	1483.9854
	ν_{18}	ν_{14}	1038.2670
	ν_{11}	ν_4	673.974 65
b_{2g}	ν_5	ν_7	990
	ν_4	ν_8	707
e_{1g}	ν_{10}	ν_{11}	847.1
e_{2u}	ν_{17}	ν_{19}	967
	ν_{16}	ν_{20}	398

dramatically reduces inhomogeneous effects. Because of the lowering of the transition dipole with increasing overtone order, these experiments are restricted to the near IR, particularly the first and second overtone bands near 6000 and 8900 cm^{-1} , respectively.^{59–61}

The spectrum of the first overtone region, reported ten years ago by Page *et al.*,^{59,60} shows the presence of at least 30 vibrational bands, spread over a range of 300 cm^{-1} (the lower panel of Fig. 1). The bright state of this transition is believed to consist of a CH stretching excitation intermediate between local and normal mode motion.⁵⁸ The multiplicity of bands mentioned above arises from the mixing of this state with a small subset of the available vibrational states. In

light of earlier theoretical studies,^{46,47} it is tempting to identify this first tier of coupled states with the states involving only in-plane vibrational modes. However, recent studies discussed in Sec. III B have shown that out-of-plane contributions cannot be neglected.

Each peak in the spectrum shown in the lower panel of Fig. 1 represents a resonance that is produced by the early time dynamics of the C–H stretch vibrational energy redistribution.

We will refer to these features as “first-order” states, to emphasize that they come from the diagonalization of the zeroth-order Hamiltonian perturbed with the strongest couplings. The survival probability calculated from this spectrum, reveals an IVR “lifetime” of the bright state of 100 fs. The qualitative features of this and other experimental spectra have been reproduced in theoretical models by Lung and Wyatt,³³ Zhang and Marcus,^{46,47} Lachello and Oss,⁶² and Rashev *et al.*⁶⁵

The experiments of Refs. 59–61 were carried out with pulsed laser sources of limited spectral resolution, which, combined with the residual inhomogeneous rotational structure present even under molecular beam conditions, lead to an effective resolution of a few cm^{-1} , limiting the study of IVR dynamics to a time scale shorter than about 1 ps.

This leaves unanswered two questions of fundamental importance for the study of reaction rates in large polyatomic molecules.

- (1) After the initially excited state has undergone the first step of IVR mixing with the in-plane modes, how much time will it take for further energy redistribution to occur? This time is equal to the lifetime that would be observed for one of the “first-order” states prepared as the initial state. Nicholson and Lawrance⁶³ have recently given a lower limit ($\tau > 21$ ps) for some of the ring modes involved, up to an energy of 8200 cm^{-1} , which

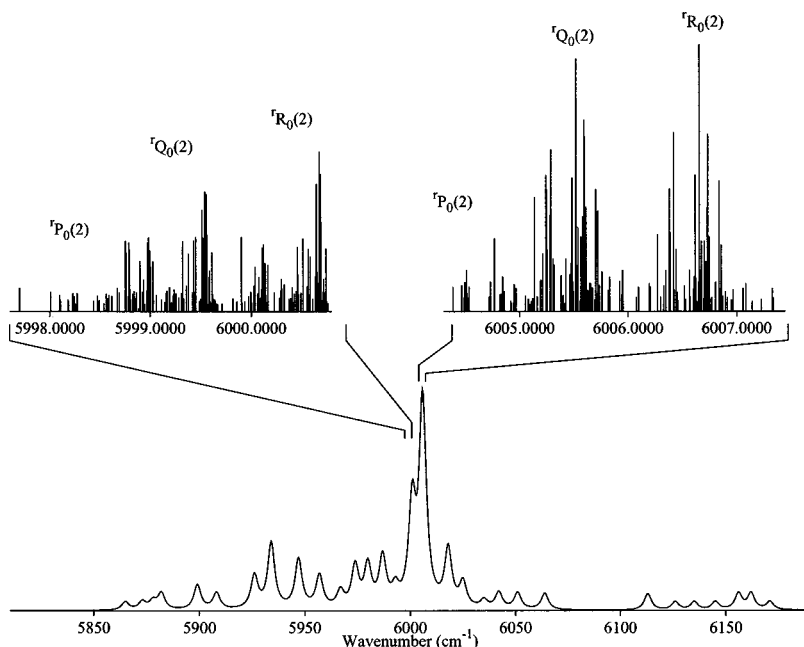


FIG. 1. The $v=2$ overtone spectrum of the CH stretch in benzene. The spectrum in the bottom panel has been reconstructed from the data of Page *et al.* (Ref. 59); the top panels are the transitions observed in this work originating from the $J=2, K=0$ ground state.

suggests that vibrational energy flow from the first tier of states into the full bath might be generally slower than previously thought.

- (2) Is this second energy redistribution complete or incomplete? Incomplete IVR implies the presence of some quantum numbers other than energy and total angular momentum that are approximately conserved in the time evolution of the bright state. Classically, this corresponds to the fact that only part of the available phase space is accessed by the trajectory originating from the initially prepared state.

The improvement in sensitivity of our molecular beam spectrometer obtained with the power buildup cavity described in Sec. II has enabled us to measure the first overtone band of benzene with full resolution of the rovibrational eigenstates thus extending the time interval over which IVR has been studied in this molecule by a factor greater than 10 000. Preliminary results have already been reported in a previous communication.⁶⁴ The congestion of the spectrum deriving from the concurrent effects of extensive fractionation of the bright state, a highly degenerate rotational structure, and small rotational constants has been overcome by using mid-IR/near-IR double resonance. This allows us to obtain the spectrum originating from a single, assigned, lower rotational level of the ground vibrational state. Therefore, having eliminated the inhomogeneous rotational structure, we have been able to unambiguously prove that it takes about 20 ps for the second step of energy redistribution to occur. Furthermore, we have also obtained evidence that full redistribution is not achieved within the time limit⁷ corresponding to the finite density of states.

II. EXPERIMENTAL APPROACH

The original version of the spectrometer along with some of the main modifications that lead to the current setup have been described before.^{15,68,69} Briefly a 1% mixture of benzene in helium is expanded in a vacuum chamber through a 50 μm nozzle at a backing pressure of 400 kPa. A 0.5 mm skimmer lets only the center portion of the free jet expansion into a second vacuum chamber, thus forming a well-collimated molecular beam. Farther downstream, the beam is then probed by a color center laser tuned in the CH overtone region. The laser interacts with the beam in a single, orthogonal crossing inside a resonant power buildup cavity (BUC) that enhances the circulating power by an estimated factor of 500 in this wavelength region. Excitation of a molecular vibration is detected by sensing the increased energy of the beam with a cryogenically cooled bolometer located downstream of the BUC.

The only significant change made to the spectrometer for this particular experiment has been to implement a double resonance scheme made necessary by the need to isolate the contribution from a single initial rotational state out of an extremely congested spectrum. A few cm downstream from the skimmer and upstream from the BUC, the beam is pumped with about 1 W of $^{13}\text{CO}_2$ laser radiation at 9.6 μm in a single—almost orthogonal—crossing. Here 1 W is enough IR power to strongly saturate the $\nu_{18}^r Q_0(2)$ transi-

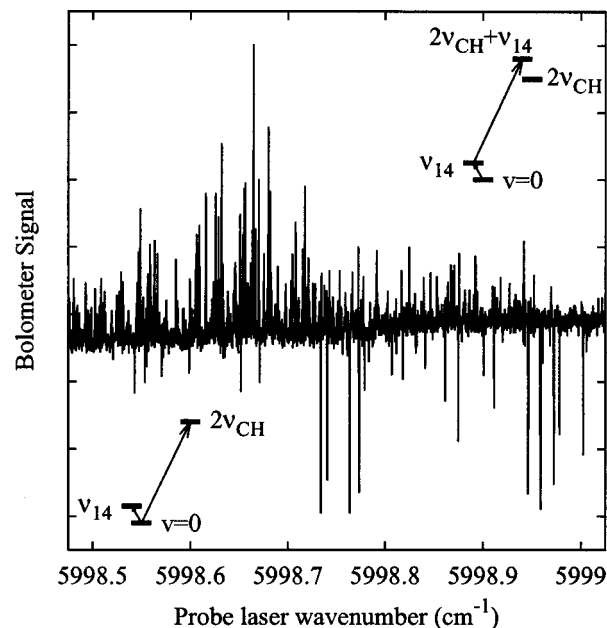


FIG. 2. The double resonance molecular beam spectrum of benzene observed with the probe laser tuned to the region of the CH stretch first overtone. Downward-going peaks correspond to transitions from the ground state, depleted by the pump laser, to the $\nu_{\text{CH}}=2$ pure overtone manifold. Upward-going peaks correspond to transitions from the upper state (ν_{18}) populated by the pump laser, to the $2\nu_{\text{CH}} + \nu_{18}$ manifold.

tion of benzene whose frequency is only 17 MHz away from the center of the R_{30} line of the $^{13}\text{CO}_2$ laser,⁵³ giving about 10 μV of signal when the laser is chopped at 280 Hz. In a single resonance spectrum an absorption signal is seen as an increase in the energy of the beam, any time the color center laser hits a molecular transition. In contrast, in a double resonance experiment a signal is seen (on top of the 10 μV baseline generated by the CO_2 laser) only when the transitions pumped by the two lasers share a common level. The signal appears as a dip in the baseline when the transitions pumped by two lasers share their *lower* state, i.e., the ground state (V-type double resonance). Alternatively the signal appears as a peak on top of the baseline if the transition pumped by the second laser originates from a ν_{18} vibrationally excited molecule, prepared by the first laser (ladder-type double resonance). Transitions of this second type (although not the main scope of this investigation) have been observed in the frequency region investigated here (Fig. 2), shifted with respect to their V-type counterparts by the cross-anharmonicity of the C–H stretching with ν_{18} .

Excess noise, due to power and frequency fluctuations of the CO_2 laser, is present in the baseline of the double resonance spectra and brings the total measured noise up to about 100 $\text{nV}/\sqrt{\text{Hz}}$ from the usual value of 40 $\text{nV}/\sqrt{\text{Hz}}$. A special problem is posed by the fact that—even if the average CO_2 laser frequency is locked to the peak of the bolometer absorption signal—occasionally large frequency excursions occur, putting the laser off resonance with the molecular transition. This causes the baseline to shift down for a short moment, which could be mistaken for a double resonance signal. The highly non-Gaussian distribution of these pseudolines, together with their observed line shapes, can be used to discriminate them from real transitions. In order to

minimize the possibility of making a mistake, two scans of each spectrum were collected under the same experimental conditions, retaining only those features that appeared in both scans.

The signal to noise ratio obtained was sufficient for the investigation of the spectrum of the strongest “first-order” feature (6005 cm^{-1} in the spectrum of Page *et al.*), but it was clear that eliminating the excess noise was needed to investigate the second most intense transition (6000 cm^{-1}) and perform a meaningful comparison between the two spectra.

We have found that the power and frequency instability of the CO_2 laser were mainly the consequence of an irregular discharge in the laser tube caused by the imperfect insulation of one of the metal plates supporting the laser tube ZnSe windows. The metal plate occasionally acted as a second cathode diverting the plasma discharge from its normal path, thus disturbing the laser action. After fixing the problem we were able to collect the spectrum of the second state (about half the intensity) with the same signal to noise. In this way it became possible for us to compare the dynamics of two different first-order states of the overtone manifold and study its dependence on the amount of CH stretching character of the bright state.

III. RESULTS AND DISCUSSION

A. Assignment and rotational state analysis

In the bottom panel of Fig. 1 the CH stretch overtone spectrum of benzene has been reconstructed from the data of Page *et al.*⁵⁹ as a sum of Lorentzian peaks. The intensity and center position of the peaks have been taken from Table I of Ref. 59, and the full width at half-maximum has been set to the value of 4 cm^{-1} reported there. The results of our high resolution investigation of the two strongest peaks is shown in the two top panels (note the 100-fold magnification of the frequency scale). We will refer to them as band A (6005 cm^{-1}) and B (6000 cm^{-1}), respectively.

We treat each of these first-order states as a separate chromophore and study the dynamics that each would have, if separately prepared as the initial state (e.g., by a short laser pulse of appropriate spectral width). This description is appropriate, as long as there is a separation of time scales in the IVR dynamics, which is indeed the case here. These first-order states do not necessarily coincide with a pure CH stretch anymore, as a result of the mixing caused by the early IVR dynamics.

Each of the two bands is composed of more than 200 lines, which must be assigned to a complete set of quantum numbers before proceeding with the analysis of the underlying dynamics. Since these are V-type double resonance spectra, all observed transitions must originate from the $J=2$, $K=0$ ground state labeled by the CO_2 laser. This, in conjunction with the selection rules $\Delta J=0, \pm 1$ and $\Delta K=\pm 1$ for a perpendicular band, restricts the candidates for an assignment to three transitions only: ${}^rR_0(2)$, ${}^rQ_0(2)$, and ${}^rP_0(2)$ corresponding to the upper rotational states $J'_K = 3_1, 2_1, 1_1$, respectively. Lines corresponding to all three possible transitions are visible in the spectra as three partially overlapping clumps: ${}^rR_0(2)$ and ${}^rQ_0(2)$ with about the same

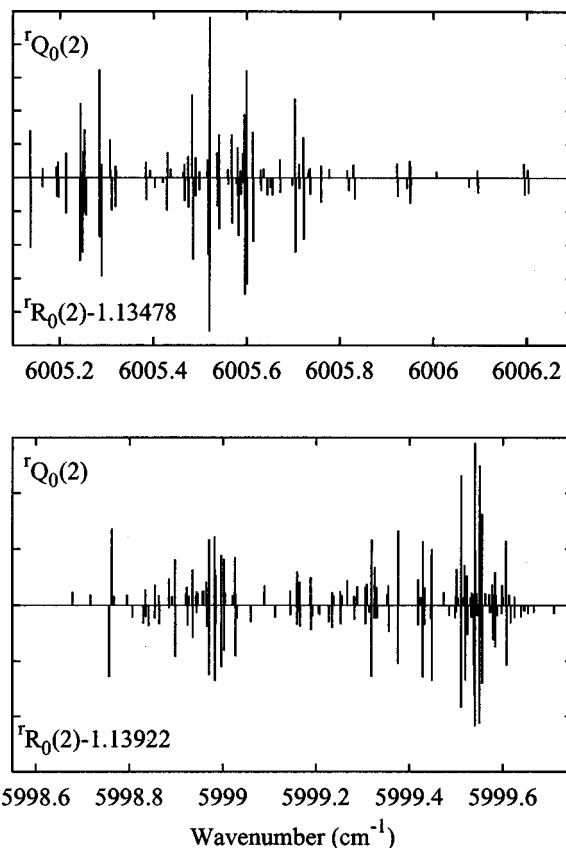


FIG. 3. A comparison between the different transitions originating from the same ($J=2$, $K=0$) lower state observed in the eigenstate resolved spectrum. The R branch lines (downward) are made to approximately coincide with the corresponding ones in the Q branch by shifting them down by 1.13478 and 1.13922 cm^{-1} , respectively.

relative intensity and ${}^rP_0(2)$ with about $1/4$ relative intensity. (This ratio is erroneously reported as $1/3$ in our first paper.⁶⁴) For single resonance spectra, Hönl–London factors give a 1:5:4 intensity ratio for the P , Q , and R transitions, respectively. For double resonance spectra, some corrections apply, depending on the relative polarization and the degree of saturation of the two transitions.⁷⁰ Given that in our experiment the degree of saturation of the first transition and the relative laser polarization are both uncontrolled parameters, the observed intensities can be considered, in agreement with the expected ones.

Since there is no ambiguity in the notation we will often refer to these clumps just as the R , Q , and P clumps, respectively. Because of the lower relative intensity of the P branch, several of its weaker transitions have probably disappeared into the noise, and, in fact, only about 60% of the lines observed in the Q or R branches have a counterpart in the P branch. Therefore, unless otherwise specified, the lines of the P clumps have not been used for quantitative analysis. A preliminary assignment of each observed line to $J'=1, 2$, or 3 has been made simply by visual inspection of the relative intensities and line positions. The assignment has been checked and—in the regions where two clumps overlap—refined by a direct comparison between P , Q , and R branches as shown in Fig. 3 for the R and Q branches.

The procedure is, in principle, rigorously justified only

when transitions to the same final state are compared, or when the IVR and rotational dynamics are completely separable, i.e., the interaction between vibrations and rotations is negligible in comparison to the interaction between the vibrations themselves. Although the final J is not the same here, the similarities observed between different rotational levels (see Fig. 3) point to the fact that—at least for the low J states studied here—the IVR dynamics is strongly dominated by anharmonic coupling with a negligible contribution from Coriolis coupling. It is also quite clear from the comparisons that the position of the bath states involved in the dynamics is not much different at $J=3$ than at $J=2$, which, in turn, implies that these bath states have similar rotational constants. The degree of similarity is an important parameter since it is related to the ergodicity (or lack thereof) of the dynamics, as discussed below. It can be quantified by calculating the standard deviation $\sigma_{2,3}$ of the frequency difference between pairs of corresponding lines in ${}^rQ_0(2)$ and ${}^rR_0(2)$. We assume that the bath states in the energy region under investigation have rotational constants $B' = B'' + \Delta B$, where B'' is the ground state rotational constant and ΔB is normally distributed with variance σ_B . Then, indicating with $\langle \rangle$ the average over all pairs:

$$\begin{aligned}\sigma_{2,3} &= \sqrt{\langle (\Delta B)^2 [J(J+1)_{J=3} - J(J+1)_{J=2}]^2 \rangle} \\ &= 6 \sqrt{\langle (\Delta B)^2 \rangle} = 6\sigma_B.\end{aligned}\quad (1)$$

Unfortunately the procedure is to some extent arbitrary, since it is not necessary that all the lines in one branch have a clear counterpart in the other, and, in fact, some of them actually do not have one. To simply disregard these lines is likely to give an underestimate of the actual value of $\sigma_{2,3}$, while just pairing them with the closest available match is likely to give an overestimate. A reasonable compromise, often used in statistical data analysis, is to calculate $\sigma_{2,3}$ with the latter procedure, discard the pairs whose mismatch is larger than $3\sigma_{2,3}$ and then recalculate $\sigma_{2,3}$.

The value $\sigma_B = 5.0 \times 10^{-4}$ and $4.1 \times 10^{-4} \text{ cm}^{-1}$ thus obtained for the A and B band, respectively, can be compared with the corresponding variance of ΔB for the bath states in the C–H stretch fundamental region, to check if the more than 100-fold increase in the density of vibrational states going from the fundamental to the overtone region produces an increased degree of mixing between the states. If the bath states have the same degree of mixing in the fundamental as in the overtone region then the value of σ_B for the overtone should be twice the value for the fundamental. This arises from the fact that (see Ref. 71, p. 400) for a state with v_1, v_2, \dots, v_n quanta in mode $1, 2, \dots, n$:

$$\Delta B = - \sum \alpha_i v_i, \quad (2)$$

and states in the CH stretch overtone energy region have, on average, twice as many vibrational quanta as those in the fundamental. Conversely, if mixing of the bath states increases significantly going from the fundamental to the overtone, then their rotational constants are equalized by the mixing and the increase of σ_B is smaller than the twofold value expected. Remarkably, the value of $2.1 \times 10^{-4} \text{ cm}^{-1}$ esti-

ated for σ_B in the CH fundamental region from the 20 perturbing states observed by Pliva and Pine⁵⁰ speaks, unexpectedly, in favor of unchanged mixing.

B. IVR dynamics

Once the lines in the spectrum have been assigned according to their J, K quantum numbers, it is possible to start analyzing the underlying dynamics. Most of the following analysis (in particular, the level spacing statistics) would be severely biased if the finite signal to noise would cause too many of the weakest transitions to disappear into the noise, preventing their observation. Therefore the first quantity that we want to analyze and compare to the expected value is the observed density of coupled states. The expected density of coupled states has been calculated from the inverse Laplace transform of the partition function⁷² in the harmonic approximation using the fundamental frequencies of Table I. The harmonic approximation clearly underestimates the actual density of states. However, for the low average number of quanta in each mode typical of the energy region investigated, it has been estimated⁷³ that the error is less than 10%. For benzene, we estimate a worse-case error by neglecting the CH stretch anharmonicity and placing the overtone 100 cm^{-1} higher, at 6100 cm^{-1} . At this energy the calculated density of states is larger by 16%, which is clearly an overestimate, since the CH stretch has the largest anharmonicity among all the modes and since the average number of quanta per mode is low. In light of this, even a 10% error is still a safe estimate.

Of the calculated 1600 states/ cm^{-1} at the energy of 6000 cm^{-1} , on average about 1/12 ($\rho_{\text{calc}} = 133/\text{cm}^{-1}$) have the right e_{1u} symmetry to couple to the bright state.⁷⁴

The observed density of coupled states can be calculated as

$$\rho_{\text{obs}} = (N-1)/\Delta E, \quad (3)$$

where N is the number of states observed and ΔE the energy range they occupy. In all cases the value obtained is low but, at least for the Q and R branches, at most within a factor 2 of the expected $133/\text{cm}^{-1}$, making us confident that we do see a large fraction of the coupled states. This is especially true if we limit ourselves to the center portions of the clumps where the intensity is higher and less lines are likely to be lost into the noise. Furthermore, the statistical analysis of level spacing carried out in the next section give values of the average density of states in accordance with those calculated here. For both A and B bands ρ_{obs} does not depend appreciably on J , which confirms the initial impression that Coriolis coupling does not play a significant role in the dynamics, at least for the low- J states investigated here.

An important question to answer is the following: what would be the lifetime of the first-order bright state if we were to prepare it at $t=0$ with, say, a short laser pulse? To estimate the IVR rate k_{IVR} , we have chosen the Fermi golden rule:

$$\Gamma_{\text{IVR}} = 2\pi \langle V^2 \rangle \rho, \quad (4)$$

$$k_{\text{IVR}} = \Gamma_{\text{IVR}}/\hbar, \quad (5)$$

TABLE II. Average properties of the IVR multiplets observed in the CH stretching overtone spectrum of benzene. The multiplets are labeled with the rotational quantum number J and energy of their parent bright state E_b : average coupling ($\langle V \rangle$) and total square of the coupling ($\sum V_i^2$) to the bath, number (N_d) and density ρ_{obs} of observed coupled states, and the lifetime from Fermi's golden rule (τ_{GR}). The density of states calculated with the statistical methods of Sec. III C, ρ_{app} , is also listed for comparison.

J'	E_b cm^{-1}	N_d	$\langle V \rangle$ 10^{-2}cm^{-1}	$\sum V_i^2$ $(10^{-2} \text{cm}^{-1})^2$	ρ_{obs} states/ cm^{-1}	ρ_{app} states/ cm^{-1}	τ_{GR} ps
1	5998.54434	32	5.18	858	30		10
2	5999.32159	79	2.89	659	88	85	11
3	6000.42639	98	2.72	725	104	107	11
1	6004.72700	36	3.53	448	49		14
2	6005.50787	71	2.63	491	67	68	18
3	6006.63914	62	2.65	435	59	59	20

with the value of ρ given by Eq. (3) and that of $\langle V^2 \rangle$, the average squared matrix coupling element, given by the result of a Lawrance–Knight deconvolution of the spectrum.⁷⁵ When, as in our case, V and ρ are given in cm^{-1} and $\text{states}/\text{cm}^{-1}$, respectively, the equations above give

$$k_{\text{IVR}} = 4\pi^2 \langle V^2 \rangle \rho c. \quad (6)$$

This method is not as self-evident as fitting an exponential decay to the survival probability obtained from the Fourier transform of the spectrum autocorrelation function (see below). However, it has the advantage of giving a more robust estimate of the actual rate, since the estimated rate calculated from spectral autocorrelation can change significantly, depending on which portion of the initial decay is used for the fit. The values obtained from Fermi's golden rule are reported in Table II.

In all cases the lifetimes range from 10 to 20 ps, which is almost one order of magnitude longer than the estimate given by Page *et al.*,^{59,60} based on the linewidth of the peaks in their spectrum and clearly limited by their finite laser resolution. Quite remarkably, the observed lifetimes are comparable to the lower limit ($\tau > 21$ ps) determined by Nicholson and Lawrance⁶³ for the ring modes $n\nu_1 + 2\nu_6$ ($n = 0 \rightarrow 7$) up to 8200 cm^{-1} . This agreement suggests a two step IVR process for the C–H stretching overtone. In the first step (≈ 100 fs), the initial excitation is rapidly redistributed among a first tier of states—which includes the $n\nu_1 + 2\nu_6$ ring modes—producing the spectrum observed by Page and co-workers. Then, in a second, slower step (≈ 10 – 20 ps), further redistribution occurs into a larger bath (possibly the full bath of available states) thus producing the same linewidth observed by Nicholson and Lawrance for the ring modes. Since theoretical models^{46,47} using only a planar-benzene Hamiltonian have been able to reproduce the features of the Page *et al.* spectra, it is tempting to identify the first tier of states with the in-plane vibrations. This intuitively reasonable and physically appealing picture is, however, only a convenient approximation at best. Recent theoretical studies^{34,36–38,45} show that the out-of-plane modes also give a non-negligible contribution to the early energy redistribution. However, these same studies demonstrate that at 9.6 ps the relaxation is not complete, and that population continues to flow into certain low frequency modes on this time scale or longer.

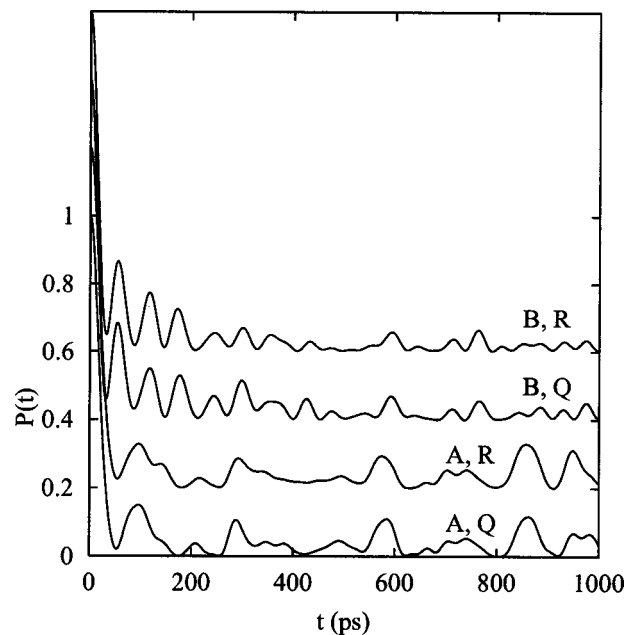


FIG. 4. The survival probability calculated from the Fourier transform of the spectrum autocorrelation function. The band termed “A” is the one observed around 6005.5 cm^{-1} ; the band termed “B” is the one observed around 5999.3 cm^{-1} . For greater clarity the plots are offset vertically by 0.2 from each other.

The survival probability (Fig. 4), calculated from the Fourier transformation of the spectral autocorrelation function:

$$P(t) = |\langle \Psi(t) | \Psi(0) \rangle|^2 = \int e^{-i\omega t} d\omega \int I(\omega') I(\omega - \omega') d\omega', \quad (7)$$

yields qualitative agreement for the lifetimes (20–25 ps) when a negative exponential is fitted to the initial decay rates, although the exact value changes by a few ps, depending on which portion of the initial decay is used for the fit.

Further inspection of the survival probability reveals that there are at least two other relevant time scales involved in the IVR process: the time for the first recurrence to occur and the time necessary for damping the recurrences. The first time scale (95 ps for band A and 55 ps for band B) is related to the substructure visible in Fig. 3, and specifically to the presence of two distinct subclumps in each J, K multiplet. This is the time that it takes for the excitation to oscillate back and forth between the two groups of states, and it is proportional to the inverse of their separation. The second is approximately the time that it would take for each of the subclumps to dephase separately and can be thought of, at this point, as the minimum time for “irreversible” decay to occur.

Another important question that we want to answer is the following: how much of the available phase space is actually sampled by the IVR dynamics? An ergodic system will sample all regions of phase space democratically in the time average, subject only to *a priori* constants of the motion.⁷⁶ One convenient measure of this degree of ergodicity is the fraction F of available states that are actually accessed.⁷

TABLE III. Fraction (F) of available states accessed by the observed IVR multiplets.

A band		B band	
$J=2$	$J=3$	$J=2$	$J=3$
0.31	0.26	0.20	0.22

$$F = \frac{N_a}{N_a^*}, \quad (8)$$

with

$$N_a^* = 2\pi^2 \langle V^2 \rangle \rho^2, \quad (9)$$

the maximum theoretical number of accessible states, and

$$N_a = \left(\sum_i p_i^2 \right)^{-1}, \quad (10)$$

the actual number of states accessed, where p_i are the normalized spectral intensities. Notice that the formula for N_a^* given in Ref. 7 is too large by a factor of 2, due to the fact that in the derivation of N_a^* [Eq. (20)] the author substitutes Γ (the full spectral width) for λ (the spectral half-width). Quantum interference limits the number of states accessed, even in the most ergodic system, to one-third of the *in principle* available states.^{7,76} Therefore, F is expected to be 1/3 for completely ergodic systems and proportionally smaller for the less ergodic ones. Notice that N_a , as defined above, is not very sensitive to weakly coupled states that are easily lost in the noise in the experimental spectrum, since they contribute very little to $\sum_i p_i^2$. That N_a^* also can be expressed in a way that is not sensitive to missing levels, becomes evident when we use the equivalent definition:

$$N_a^* = \pi \Gamma_{\text{IVR}} \rho, \quad (11)$$

which holds as long as we have a reliable estimate of the true density of states ρ . In fact, Γ_{IVR} is, roughly speaking, proportional to the spectral width and, as such, it is not very sensitive to missing levels. On the other hand, there is a larger uncertainty as to what the true density of states is. Our best estimate is the value $\rho_{\text{calc}} = 133/\text{cm}^{-1}$ calculated above, which we believe to be accurate. Table III lists the value of F thus obtained for the IVR multiplets investigated in this work. In all cases the value found is, on average, 26% lower than the expected value of 1/3 for complete relaxation, pointing to a large, but still incomplete, energy redistribution. The implications of possible errors in the estimate of the true density of states will be discussed in Sec. III D. It is important to stress here that the harmonic approximation *underestimates* the true density of states. Hence, any correction would increase ρ_{calc} and decrease the experimental value of F , ultimately giving a larger discrepancy with the 1/3 limit value.

C. Level spacing statistics

Incomplete energy redistribution from the initially prepared state implies that the bath of vibrational states into which the energy is redistributed is not a fully mixed one. Mixing destroys all approximate quantum numbers, that is

all those that—unlike, e.g., energy and total angular momentum—do not correspond to true constants of the motion. One may then wonder whether the lack of full mixing may preserve some of these approximate quantum numbers. The presence of substructure in the observed IVR multiplets, noted in Sec. III B, already implies that there are approximate quantum numbers that are preserved in the early phase of the vibrational energy redistribution. The question is whether some of these quantum numbers are still preserved on the longer time scale explored by our experiment, which is given by the resolution of the spectrometer (≈ 6 MHz) through the uncertainty principle: $\Delta t \approx 1/(2\pi \Delta \nu) \approx 25$ ns. The presence of approximate quantum numbers can be detected by the characteristic spectral features they give rise to. In the case where no good quantum numbers are left other than energy and angular momentum, all states interact with one another and mutual repulsion of the energy levels (spectral rigidity) is expected according to the Gaussian Orthogonal Ensemble model (GOE) of Dyson.²¹ Conversely, if there are approximately good quantum numbers still present, levels with different quantum numbers interact very weakly with one another. The spectrum is then formed by the superposition of several noninteracting GOE sequences (one per quantum number) and, when a large number of sequences are present, the distribution of the energy levels becomes indistinguishable from a random (Poisson) distribution.

We have tested the degree of spectral rigidity with the Δ_3 statistics of Dyson and Mehta:⁷⁷

$$\Delta_3(L) = \min_{A,B} \left(\frac{1}{L} \int_{E-L/2}^{E+L/2} [N(E) - A - BE]^2 dE \right), \quad (12)$$

which basically measures the deviation of the staircase function $N(E)$ (the number of observed levels with energy less than E) from the best fit straight line $A + BE$. The two extreme cases of a pure GOE and a pure Poisson spectrum are characterized by a remarkable difference in the L dependence of Δ_3 . Namely, when L is normalized to the average spacing, $\Delta_3 = L/15$ is expected for the Poisson and $\Delta_3 \approx 1/\pi^2 [\ln(L) - 0.0687]$ for the GOE case.

The results obtained for the Q and R branches of both the observed first-order states (see Fig. 5) point to a random (Poisson) distribution of the energy levels in all four cases. This implies that the spectrum does not consist of a single GOE sequence, but rather of several noninteracting ones, corresponding to approximately good quantum numbers that are conserved on the time scale explored by the experiment.

Before proceeding further, an important side issue must be examined. As already pointed out before, one must be careful about a possible bias introduced in the test by incomplete sequences produced by the finite signal-to-noise ratio. In order to rule out this possibility we have performed the following test: we have assumed that the spectrum actually *does* consist of a single GOE sequence of unknown density ρ_{GOE} , where only a fraction f of the levels are observed, and then checked whether the assumption is consistent with the observed spacings. Lehmann and Coy⁷⁸ give a formula for the expected level spacing distribution $P(s)$ as a function of f and $\rho_{\text{app}} = f\rho_{\text{GOE}}$ (the apparent density of states), which is used here to calculate the likelihood function:

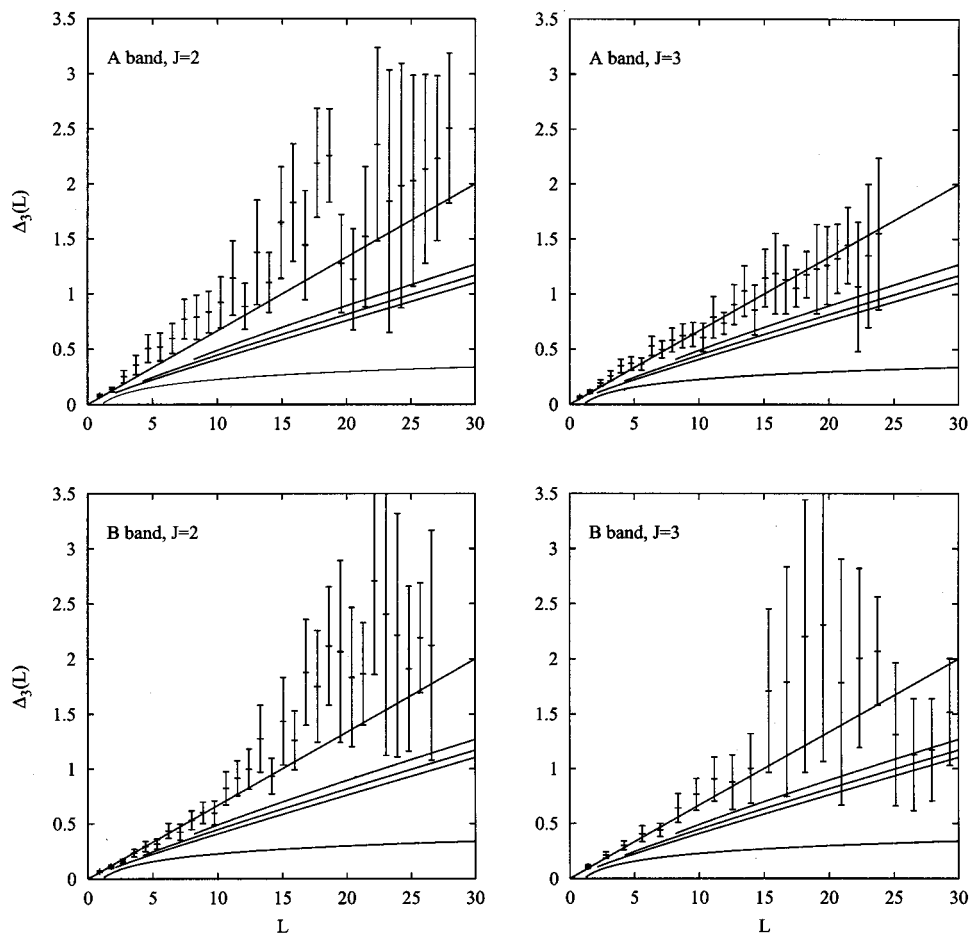


FIG. 5. Δ_3 statistics for the molecular beam spectrum of the first CH stretch overtone of benzene. The band termed ‘‘A’’ is the one observed around 6005.5 cm^{-1} ; the band termed ‘‘B’’ is the one observed around 5999.3 cm^{-1} . The solid curves plotted are, starting from the bottom, the limiting cases for (a) the single GOE sequence with no missing levels, (b) one, (c) two, and (d) four GOE sequences of equal density, of which only 50% of the levels are observed, (e) a Poisson spectrum. L is normalized to the average level spacing.

$$\mathcal{L}(\rho_{\text{app}}, f) = \prod_i P(s_i, \rho_{\text{app}}, f), \quad (13)$$

for the set of observed spacings $\{s_i\}$. As prescribed by standard statistical methods^{79,80} the best estimates \bar{f} and $\bar{\rho}_{\text{app}}$ are given by the values that maximize the likelihood function. While the confidence level of the parameters thus obtained can be quite precisely determined by bootstrapping techniques, the procedure is quite laborious and time consuming for large samples. Therefore we have chosen to use the likelihood ratio method, which, for large samples, is much faster and almost as accurate.⁸⁰

Given

$$T(\rho, f) = \frac{\mathcal{L}(\bar{\rho}_{\text{app}}, \bar{f})}{\mathcal{L}(\rho_{\text{app}}, f)}, \quad (14)$$

the quantity $-2 \ln T$ follows, in the limit of large samples, a χ^2 distribution with one degree of freedom. The confidence region at the level α for the parameters is then simply given by the set of parameters that satisfy the relationship

$$T(\rho, f) < \chi_{1-\alpha}^2, \quad (15)$$

where $\chi_{1-\alpha}^2$ is defined such that

$$P(\chi^2 > \chi_{1-\alpha}^2) = \alpha. \quad (16)$$

The results obtained are shown in Fig. 6 and reported in Table IV with their 1σ confidence intervals. It is evident that if the hypothesis being tested is true, the real density of bath

states not only must be much higher than the ρ_{calc} value calculated before for the density of vibrational states of e_{1u} symmetry ($133/\text{cm}^{-1}$), but also must be higher than the $(2J+1)\rho_{\text{calc}}$ value expected in the case of complete breakdown of the K symmetry, produced by Coriolis coupling, the presence of which is, in any case, not detected in the spectra (see above). Therefore, there is strong evidence that under no reasonable circumstances is the hypothesis of a single sequence compatible with the observed spectra, and hence it must be rejected.

Unfortunately, determining the exact number of sequences present in the spectrum is not possible, given the limited number of states observed. An estimate can be found, however, based on the above conclusion that at least 50% of the states are actually observed, and on the following simple consideration. For a spectrum composed of several arbitrary GOE sequences, each with fractional density ρ_i :⁸¹

$$\Delta_3(L) = \sum \Delta_3(\rho_i L)_{\text{GOE}}. \quad (17)$$

When only a fraction of the actual levels f is, on average, observed, each term of the sum in Eq. (17) is proportionally reduced. On the other hand, a new term arises from the ‘‘random’’ disappearance of the remaining $1-f$ fraction of levels (see the Appendix). This gives

$$\Delta_3(L) = (1-f) \frac{L}{15} + f^2 \sum \Delta_3\left(\frac{\rho_i L}{f}\right)_{\text{GOE}}, \quad (18)$$

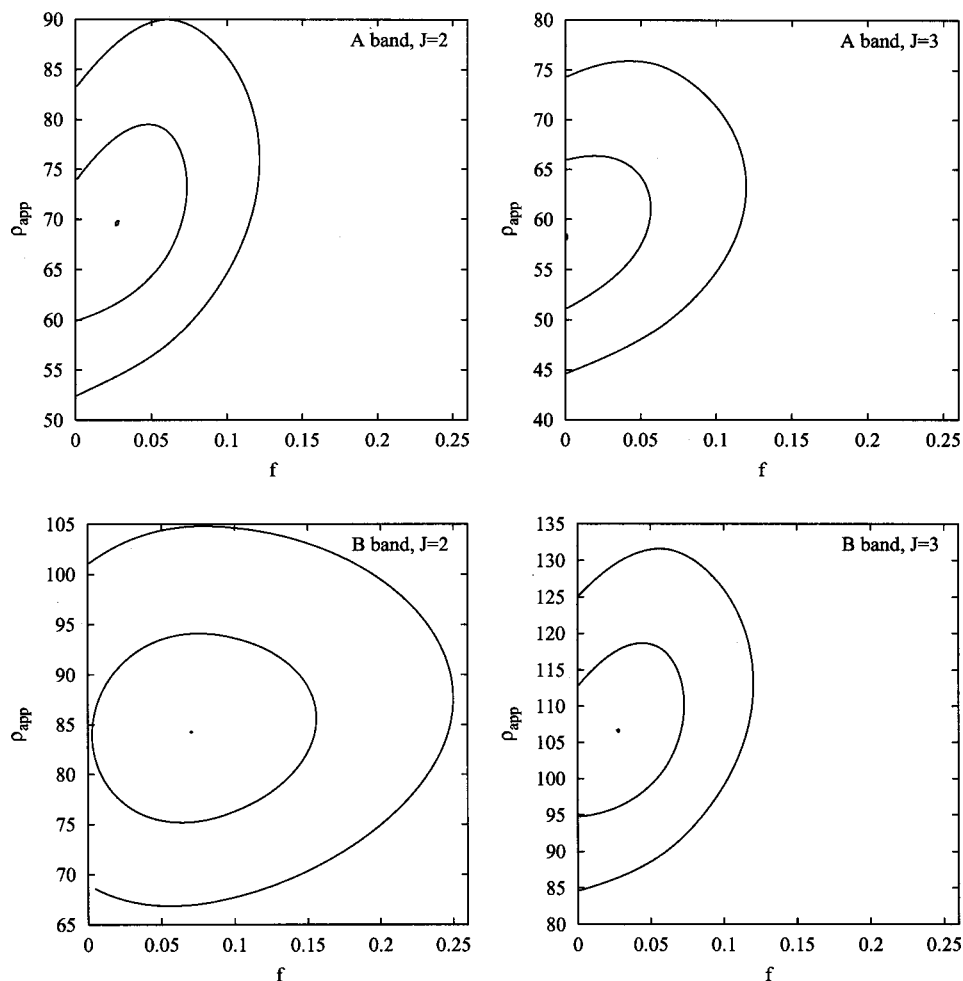


FIG. 6. Confidence regions for the hypothesis that the observed benzene overtone spectra are composed of a single GOE sequence of density ρ , of which only a fraction f with apparent density $\rho_{\text{app}}=f\rho$ is actually observed. The band termed “A” is the one observed around 6005.5 cm^{-1} ; the band termed “B” is the one observed around 5999.3 cm^{-1} . The curves define the 1σ and 2σ confidence regions according to the likelihood function defined in Eq. (13). A small dot indicates the most probable value for the parameters. The results are also reported in Table IV.

where L is normalized to the *observed* average spacing.

Since in all cases the observed Δ_3 (Fig. 5) does not deviate from the $L/15$ line up to $L=25$, the remaining contribution must come from the presence of several GOE sequences. As can be seen from the same figure, assuming that the GOE sequences that compose the spectrum all have the same density (the most unfavorable case), four or more independent sequences are still required to explain the observed trend.

This conclusion implies the presence of four or more conserved quantum numbers, whose nature and identity are at present unknown to us. In particular, it is not clear yet whether the sequences correspond to different values of the same quantum number, or to different quantum numbers al-

together. In general, it is not surprising to observe that the dynamics still exhibit some remnants of order. Indeed this has been previously observed for other molecules, such as NO_2 , on a time scale on the order of 200 ps.⁸² What is surprising in our case is that this happens for such a—comparatively speaking—large molecule as benzene, even on the rather long time scale (25 ns) explored by the experiment.

D. Comparison with a model calculation

In order to understand what type of Hamiltonian is compatible with, and likely responsible for, the observed features of the benzene overtone spectrum, we have performed a simple model calculation. In analogy with random matrix theory, we consider the most general Hamiltonian compatible with our *a priori* knowledge in which a single bright state is randomly coupled to a bath of dark states. The bath states zeroth-order energies are drawn from a uniform distribution centered on the bright state energy, with a density $\rho = \rho_{\text{calc}} = 133/\text{cm}^{-1}$. The couplings between the bright state and each of the bath states in turn are drawn from a Gaussian random distribution with zero mean and standard deviation $\bar{V} = 2.1 \times 10^{-2}\text{ cm}^{-1}$, such that $\Gamma = 2\pi\bar{V}^2\rho$ is equal to the average Γ_{IVR} for the four multiplets analyzed. Couplings between each pair of bath states are drawn from a Gaussian random distribution with zero mean and standard deviation

TABLE IV. Parameters corresponding to the maximum of the likelihood function of Eq. (13) for the observed spectra of benzene. Densities of states (ρ) are given in states/ cm^{-1} . The uncertainties given are one standard deviation.

	A band		B band	
	$J=2$	$J=3$	$J=2$	$J=3$
f	<0.07	<0.05	<0.15	<0.07
ρ_{app}	68 ± 8	59 ± 7	85 ± 9	107 ± 12
ρ_{GOE}	>970	>1180	>560	>1500
$(2J+1)\rho_{\text{calc}}$	665	931	665	931

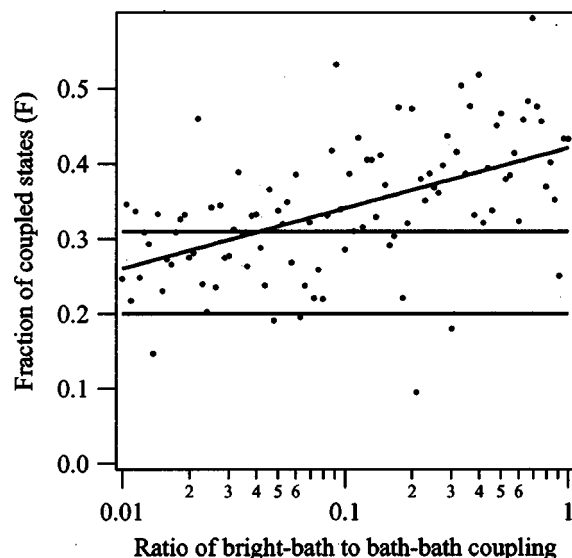


FIG. 7. The calculated fraction (F) of available states accessed by the IVR dynamics as a function of the bright state–bath to bath–bath coupling ratio. Thin lines show the result of a pseudolinear fit and the 1σ confidence bands. The thick lines show the region compatible with the range of values of F observed experimentally.

\bar{W} , which is kept as an adjustable parameter. In order to minimize edge effects, we start with 400 bath states, diagonalize the corresponding Hamiltonian and retain only the 200 central eigenstates to calculate Δ_3 and F (see above). The results of this model calculation are summarized in Figs. 7 and 8. Figure 7 shows the value of F for synthetic spectra generated with \bar{W}/\bar{V} varying from 0.01 to 1 in 5% increments. As expected, the average value of F increases with increasing bath–bath coupling, but with visibly large fluctuations about the average. These large fluctuations prevent the exact pinpointing of the extent of bath–bath coupling that corresponds to the values of F of the observed spectra. In

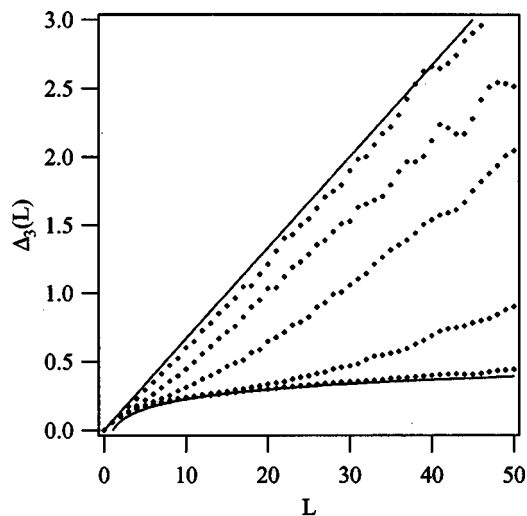


FIG. 8. Calculated Δ_3 statistics for different ratios of the bright state–bath (\bar{V}) to bath–bath (\bar{W}) coupling. From top to bottom: ($\bar{W}/\bar{V}=0, 0.1, 0.2, 0.5, 1$). Each point corresponds to the average of $\Delta_3(L)$ over 20 randomly generated spectra. Solid lines are the limits expected for Poisson and GOE spectra, respectively.

spite of this, Fig. 7 justifies the belief that the ratio of bright–bath to bath–bath coupling must likely be smaller than 0.2. More compelling evidence comes from the results presented in Fig. 8, where $\Delta_3(L)$ is plotted for $\bar{W}/\bar{V}=0, 0.1, 0.2, 0.5, 1$. Again, a comparison with the experimental results (Fig. 5) shows that the observed spectral features are incompatible with a strong bath–bath coupling, i.e., with \bar{W}/\bar{V} ratios higher than 0.2.

It is important to remark here that the Δ_3 and F statistics lead to the same result in two complementary ways. As we have remarked earlier, Δ_3 statistics give useful information only when a substantial fraction of the coupled states are observed, which we believe to be the case, based on our estimate of the density of states. However unlikely, complete breakdown of the K rotational symmetry and anharmonic interaction, which we have neglected in our treatment, could give rise to a much more dense bath than expected, thus making the result of the Δ_3 analysis unusable. On the other hand, the F statistics remains valid, as discussed, as long as the appropriate density of states is used in Eq. (11). It is clear from the previous discussion that an increased density of states would proportionally decrease the value of F for the experimentally observed spectra, thus pointing even more strongly to a weakly coupled bath.

The question arises then as to what is the physical reason why the bright state is more strongly coupled to the bath than the bath states are among themselves. Giving a definite answer without the support of accurate—and time consuming—calculations is very difficult or perhaps impossible. There is, nevertheless, a simple and often overlooked argument that could prove this apparently counterintuitive phenomenon to be the rule rather than the exception.

It is well known that the coupling matrix elements between two vibrational states on average decrease exponentially with the order of the term in the Hamiltonian expansion that connects the two states, that is, with the “distance” in quantum number between the two states.^{23,83–85} Perhaps less obvious, the state for which all the energy is in the highest frequency mode has—at least in the limit of a system with an infinite number of vibrational modes—a unique property among the set of states in the same energy shell: its “distance” from a state taken at random from the set is, on average, the shortest. If—as in the present case—the bright state corresponds to the highest-frequency mode, one would then find it normal for the bright state–bath coupling to be stronger than the bath–bath coupling. That the minimum “distance” property holds for the bright state thus defined follows from two facts.

- (i) In a system with an infinite number of vibrational modes at a given energy, the probability that two states taken at random have nonzero quanta in the same vibrational mode is zero. Then the “distance” between these two states is simply the sum of their total number of vibrational quanta.
- (ii) Since the bright state has the highest frequency, it also has the smallest number of total vibrational quanta for a given energy.

Then, with n_b the number of quanta in the bright state

(two in the case of benzene) and $n_d (> n_b)$ the average number of quanta in the bath, the average bright state–bath distance is $n_b + n_d$, which is smaller than the average bath–bath distance $2n_d$.

The above reasoning also holds for finite systems, as long as the average number of quanta per mode is much smaller than 1. Unfortunately, in benzene at 6000 cm^{-1} this approximation fails for the lowest-frequency modes. An additional complication arises from the fact that couplings decrease exponentially with the distance in quantum number. This implies that the average coupling is sensitive to the tail of the distribution of distances on the short distance side, and one needs to know not only the average but also the width of the distribution. In order to overcome these problems, we have adopted the more robust choice of computing the bright state–bath and bath–bath distance distribution directly from the list of vibrational states in the energy region of interest, calculated in the approximation of harmonic frequencies. Since generating all the vibrational states in the 6000 cm^{-1} region is a very time consuming task, we have randomly picked a suitable subset of them. The procedure is simple and quite convenient for all the situations where the total number of vibrational states is too large to handle: for each state in the subset the number of quanta in each vibrational mode is randomly chosen from a Boltzmann distribution with a fictitious temperature T_0 . When the appropriate T_0 is chosen, the energy of the states chosen with this method is strongly peaked at the energy of interest, and states in the same energy shell have the same probability of being randomly picked. Therefore the states chosen are an unbiased subset of the full collection of states in which we are interested. The energy distribution can be narrowed down, if needed, without introducing any bias by simply discarding states with total energy outside a prescribed window.

The definition of distance between two modes in a molecule with degenerate vibrational modes requires a little care. It is convenient for this purpose to use symmetrized vibrational coordinates^{39,65} and label the states with the number of quanta in each symmetrized coordinate: $\{n_i\} = (n_1, n_2, \dots, n_{30})$. In this way each $\{n_i\}$ has a well-defined (complex) symmetry and the distance between two states $\{m_i\}$ and $\{n_i\}$ is simply $\sum_i |m_i - n_i|$.

For our calculation we have used $kT_0 = 606\text{ cm}^{-1}$ and kept only states that fall in the $5800\text{--}6200\text{ cm}^{-1}$ energy window. Figure 9 shows the distribution of distances, respectively, between the bright state and 10 000 randomly chosen bath states and between 10 000 couples of randomly chosen bath states. For the sake of convenience we have disregarded the symmetry of the states, that is, we have assumed that all the chosen states belong to the same symmetry class as the bright state. This should not introduce any approximation as long as the distribution of distances is the same for all symmetry classes. It is evident from the plot that the average bright state–bath distance is smaller by about two quanta than the average bath–bath distance. Furthermore, even for shorter distances, the curve for the bright state remains above or comparable to the distribution for the bath–bath distance. An additional contribution could come from the fact that anharmonic coupling is generally stronger for states with all

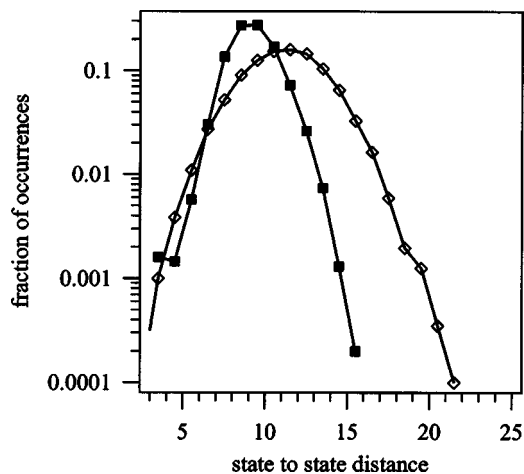


FIG. 9. The distribution of the bright state–bath (filled squares) and bath–bath (unfilled diamonds) distance (in vibrational quantum number space) for 20 000 randomly selected states at $\approx 6000\text{ cm}^{-1}$. Note that the distances are discrete values, and the lines serve only as a guide to the eye. Note also the vertical log scale.

quanta in a single mode (like our bright state) than it is for states with small numbers of quanta in each mode.⁸⁶

IV. SUMMARY AND CONCLUSIONS

An analysis of the eigenstate resolved spectrum of benzene in the region of the first C–H stretching overtone, joined by a comparison with previously reported results, reveals a highly nonergodic energy redistribution dynamics involving several different time scales. The secondary time scales observed are much longer than the 100 fs previously observed for the primary IVR time scale of the CH stretching vibration. The dynamics appears dominated by anharmonic coupling, with little or no contribution from Coriolis coupling. The time necessary for secondary energy redistribution ($\approx 10\text{--}20\text{ ps}$), which is comparable with the estimate of Nicholson and Lawrance for the relaxation of ring modes up to 8200 cm^{-1} suggests a two step process, with fast redistribution to a first tier of states and subsequent slow redistribution to the complete bath. Level spacing statistics reveal that the dynamics produces—even at an “infinite time”—a highly mixed, but not statistical, distribution of vibrational excitation. We have shown how this incomplete IVR is likely to originate from a bath–bath coupling that is much weaker than the bright state–bath coupling. We propose that this nonintuitive feature could be typical of large molecules whenever the bright state vibrational energy is localized in a high-frequency mode.

The results obtained show the power of eigenstate resolved molecular beam spectroscopy as a tool for studying intramolecular vibrational energy redistribution in relatively large molecules. We have also shown how the information provided by eigenstate resolved spectra is not limited to the IVR of the bright state. When the appropriate estimators are used, eigenstate resolved spectra can provide useful information about bath–bath couplings (hence about their IVR) using the bright state IVR as a clock. These results also show how statistical methods nicely complement “exact” Hamil-

tonian analysis (discussed, e.g., in Ref. 87) in extracting dynamical information from frequency resolved spectra. While exact methods give the most detailed information and are as such, preferable whenever possible, often the size of the molecule or the complexity of the spectra makes their applicability impossible. In this case, approximate statistical concepts become very valuable. Furthermore, these concepts being not molecule specific, they are helpful to understand the general features of IVR. In light of the results of this work, the assumptions made by RRKM and other statistical approaches for the calculation of chemical reaction rates in large polyatomic molecules should perhaps be reconsidered.

ACKNOWLEDGMENTS

We would like to thank Paul Rabinowitz for his invaluable help with the CO₂ laser, Brooks Pate and Martin Gruebele for useful discussions. Funding for this work was provided by the National Science Foundation under Grant No. CHE-97-03604. Financial support for the visit of U. M. and P. E. from the German Academic Exchange Service (DAAD) is gratefully acknowledged.

APPENDIX: Δ_3 STATISTICS FOR MULTIPLE, INCOMPLETE SEQUENCES

We want to prove that for a spectrum composed of several arbitrary GOE sequences, each with fractional density ρ_i , when only a fraction of the actual levels f is, on average, observed:

$$\Delta_3(L) = (1-f) \frac{L}{15} + f^2 \sum_i \Delta_3 \left(\frac{\rho_i L}{f} \right) \text{GOE}, \quad (\text{A1})$$

where L is normalized to the *observed* average spacing. A similar formula is given by Mukamel, Sue, and Pandey⁸⁸ without proof. Note that Ref. 88 uses a different notation: there f is the fraction of *missing* levels, and $1-f$ is the fraction of *observed* levels.

Let us indicate with a primed symbol the actual (unknown) value of a parameter and with unprimed symbols the observed value. Thus L' and $L = fL'$ will be the length of an interval in average spacings (true and observed spacing, respectively), n' the number of actual levels in a given interval and n the number of observed levels in the same interval.

We start by considering the variance $\Sigma^2(L') = \langle n'^2 \rangle - \langle n' \rangle^2$ of the number of levels observed in an interval of length L' . For a single GOE sequence with no missing levels:³⁰

$$\Sigma_G^2(L') = \frac{2}{\pi^2} [\ln(2\pi L') + a], \quad (\text{A2})$$

with $a = \gamma + 1 - \pi^2/8$.

To treat the case of a single sequence with missing levels, we first need to find the probability $P_f(L', n)$ of observing n levels in an interval of length L' , when every level in the interval has a probability f of being observed. This is given by

$$P_f(L', n) = \sum_{n'} P(f, n, n') P_G(L', n'), \quad (\text{A3})$$

where $P_G(L', n')$ is the probability that a perfect GOE sequence has n' levels in a given interval of length L' and $P(f, n, n')$ is the probability of observing n of these n' levels when each individual level has a probability f of being observed. The latter is given by the binomial distribution:

$$P(f, n, n') = f^n (1-f)^{(n'-n)} \binom{n'}{n}. \quad (\text{A4})$$

Then

$$\begin{aligned} \langle n \rangle_{f, L'} &= \sum_n n P_f(L', n) \\ &= \sum_n \sum_{n'} n P(f, n, n') P_G(L', n'), \end{aligned} \quad (\text{A5})$$

changing the order of summation gives

$$\begin{aligned} \langle n \rangle_{f, L} &= \sum_{n'} \sum_n n P(f, n, n') P_G(L', n') \\ &= \sum_{n'} f n' P_G(L', n') = f \langle n' \rangle_{G, L'}, \end{aligned} \quad (\text{A6})$$

with $\langle n \rangle_{G, L}$ the average number of levels in an interval of length L for a perfect GOE sequence.

Similarly,

$$\begin{aligned} \langle n^2 \rangle_{f, L'} &= \sum_n n^2 P_f(L', n) \\ &= \sum_n \sum_{n'} n^2 P(f, n, n') P_G(L', n') \end{aligned} \quad (\text{A7})$$

$$\begin{aligned} &= \sum_{n'} \sum_n n^2 P(f, n, n') P_G(L', n') \\ &= \sum_{n'} f n' (1-f + f n') P_G(L', n') \end{aligned} \quad (\text{A8})$$

$$= f(1-f) \langle n' \rangle_{G, L'} + f^2 \langle n'^2 \rangle_{G, L'}. \quad (\text{A9})$$

Substituting in

$$\Sigma_f^2(L') = \langle n^2 \rangle_{f, L'} - \langle n \rangle_{f, L'}^2, \quad (\text{A10})$$

gives

$$\Sigma_f^2(L') = f(1-f) \langle n' \rangle_G + f^2 (\langle n'^2 \rangle_G - \langle n' \rangle_G^2) \quad (\text{A11})$$

$$= f(1-f) L' + f^2 \Sigma_G^2(L'), \quad (\text{A12})$$

which can be written as

$$\Sigma_f^2(L) = (1-f)L + f^2 \Sigma_G^2(L/f). \quad (\text{A13})$$

Substituting the above formula in the definition³⁰

$$\Delta_3(L) = 2/L^4 \int_0^L (L^3 - 2L^2 R + R^3) \Sigma^2(R) dR, \quad (\text{A14})$$

gives

$$\Delta_3(L)_f = (1-f)L/15 + f^2 \Delta_3(L/f). \quad (\text{A15})$$

If the n' level in a given interval comes from i different GOE sequences n_1, n_2, \dots, n_i with $n_1 + n_2 + \dots + n_i = n$, the hypothesis of statistical independence gives

$$\Sigma_G^2(L') = \sum 2/\pi^2 [\ln(n'_i) + a], \quad (\text{A16})$$

and the same calculation performed above for a single sequence gives the desired result:

$$\Delta_3(L)_f = (1-f)L/15 + f^2 \sum_i \Delta_3(\rho_i L/f). \quad (\text{A17})$$

- ¹N. B. Slater, *Theory of Unimolecular Reactions* (Cornell University Press, Ithaca, NY, 1959).
- ²R. A. Marcus and O. K. Rice, *J. Phys. Colloid Chem.* **55**, 894 (1951).
- ³R. A. Marcus and O. K. Rice, *J. Chem. Phys.* **20**, 359 (1952).
- ⁴H. M. Rosenstock, M. B. Wallenstein, A. L. Wahrhaftig, and H. Eyring, *Proc. Natl. Acad. Sci. U.S.A.* **38**, 667 (1952).
- ⁵T. Baer and W. L. Hase, *Unimolecular Reaction Dynamics* (Oxford University Press, New York, 1996).
- ⁶K. A. Holbrook, M. J. Pilling, and S. H. Robertson, *Unimolecular Reactions*, 2nd ed. (Wiley, Chichester, 1996).
- ⁷E. J. Heller, *J. Chem. Phys.* **92**, 1718 (1990).
- ⁸A. M. de Souza, D. Kaur and D. S. Perry, *J. Chem. Phys.* **88**, 4569 (1988).
- ⁹G. A. Bethardy and D. S. Perry, *J. Chem. Phys.* **98**, 6651 (1993).
- ¹⁰K. von Puttkamer, H.-R. Dübal, and M. Quack, *Faraday Discuss. Chem. Soc.* **75**, 197 (1983).
- ¹¹Quack, *Annu. Rev. Phys. Chem.* **X**, 839 (1990).
- ¹²M. Quack and J. Stohner, *J. Phys. Chem.* **97**, 12 574 (1993).
- ¹³K. K. Lehmann, B. H. Pate, and G. Scoles, *J. Chem. Phys.* **93**, 2152 (1990).
- ¹⁴K. K. Lehmann, B. H. Pate, and G. Scoles, in *Mode Selective Chemistry*, edited by J. Jortner *et al.* (Kluwer Academic, Dordrecht, 1991), pp. 17–23.
- ¹⁵E. R. T. Kerstel, K. K. Lehmann, T. F. Mentel, B. H. Pate, and G. Scoles, *J. Phys. Chem.* **95**, 8282 (1991).
- ¹⁶J. E. Gambogi, K. K. Lehmann, B. H. Pate, G. Scoles, and X. Yang, *J. Chem. Phys.* **98**, 1748 (1993).
- ¹⁷A. A. Stuchebrukhov and R. A. Marcus, *J. Chem. Phys.* **98**, 6044 (1993).
- ¹⁸M. Bixon and J. Jortner, *J. Chem. Phys.* **48**, 715 (1968).
- ¹⁹K. G. Kay, *J. Chem. Phys.* **64**, 2112 (1976).
- ²⁰K. G. Kay, *J. Chem. Phys.* **61**, 5205 (1974).
- ²¹F. J. Dyson, *J. Math. Phys.* **3**, 140 (1962).
- ²²E. W.-G. Diau, J. L. Herek, Z. H. Kim, and A. H. Zewail, *Science* **279**, 847 (1998).
- ²³M. Gruebele and R. Bigwood, *Int. Rev. Phys. Chem.* **17**, 91 (1998).
- ²⁴J. Segall, R. N. Zare, H. R. Dübal, M. Lewerenz, and M. Quack, *J. Chem. Phys.* **86**, 634 (1987).
- ²⁵L. Lubich, O. V. Boyarkin, R. D. F. Settle, D. S. Perry, and T. R. Rizzo, *Faraday Discuss.* **102**, 167 (1995).
- ²⁶O. V. Boyarkin and T. R. Rizzo, *J. Chem. Phys.* **105**, 6285 (1996).
- ²⁷D. J. Nesbitt and R. W. Field, *J. Phys. Chem.* **100**, 12 735 (1996).
- ²⁸K. K. Lehmann and G. Scoles, *Annu. Rev. Phys. Chem.* **45**, 241 (1994).
- ²⁹T. Uzer, *Phys. Rep.* **199**, 73 (1991).
- ³⁰T. Guhr, A. Müller-Groeling, and H. A. Weidenmüller, *Phys. Rep.* **299**, 189 (1998).
- ³¹K. F. Freed, *Faraday Discuss. Chem. Soc.* **67**, 231 (1979).
- ³²K. F. Freed and A. Nitzan, *J. Chem. Phys.* **73**, 4765 (1980).
- ³³C. Iung and R. E. Wyatt, *J. Chem. Phys.* **99**, 2261 (1993).
- ³⁴T. J. Minehardt and R. E. Wyatt, *Chem. Phys. Lett.* **295**, 373 (1998); **312**, 485 (1999).
- ³⁵T. J. Minehardt and R. E. Wyatt, *J. Chem. Phys.* **109**, 8330 (1998).
- ³⁶T. J. Minehardt, J. D. Adcock, and R. E. Wyatt, *Chem. Phys. Lett.* **303**, 537 (1999).
- ³⁷T. J. Minehardt, J. D. Adcock, and R. E. Wyatt, *J. Chem. Phys.* **110**, 3326 (1999).
- ³⁸T. J. Minehardt, J. D. Adcock, R. E. Wyatt, and C. Iung, *Chem. Phys. Lett.* **303**, 347 (1999).
- ³⁹S. Rashev, M. Stamova, and L. Kancheva, *J. Chem. Phys.* **109**, 585 (1998).
- ⁴⁰E. L. Sibert III, W. P. Reinhardt, and J. T. Hynes, *J. Chem. Phys.* **81**, 1115 (1984).
- ⁴¹R. E. Wyatt, C. Iung, and C. Leforestier, *J. Chem. Phys.* **97**, 3477 (1992).
- ⁴²R. E. Wyatt and C. Iung, *J. Chem. Phys.* **98**, 5191 (1993).
- ⁴³R. E. Wyatt and C. Iung, *J. Chem. Phys.* **98**, 3577 (1993).
- ⁴⁴R. E. Wyatt and C. Iung, *J. Chem. Phys.* **98**, 6758 (1993).
- ⁴⁵R. E. Wyatt, *J. Chem. Phys.* **109**, 10 732 (1998).
- ⁴⁶Y. Zhang and R. A. Marcus, *J. Chem. Phys.* **97**, 5283 (1992).
- ⁴⁷Y. Zhang and R. A. Marcus, *J. Chem. Phys.* **96**, 6065 (1992).
- ⁴⁸M. Quack, in *Mode Selective Chemistry*, edited by J. Jortner *et al.* (Kluwer Academic Publisher, Dordrecht, 1991), pp. 47–65.
- ⁴⁹P. Esherick, A. Owywong, and J. Pliva, *J. Chem. Phys.* **83**, 3311 (1985).
- ⁵⁰J. Pliva and A. S. Pine, *J. Mol. Spectrosc.* **126**, 82 (1987).
- ⁵¹H. Hollenstein, S. Piccirillo, M. Quack, and M. Snels, *Mol. Phys.* **71**, 759 (1990).
- ⁵²J. Domenech, M.-L. Junttila, and A. S. Pine, *J. Mol. Spectrosc.* **149**, 391 (1991).
- ⁵³M. L. Junttila, J. L. Domenech, G. T. Fraser, and A. S. Pine, *J. Mol. Spectrosc.* **147**, 513 (1991).
- ⁵⁴M. Snels, A. Beil, H. Hollenstein, and M. Quack, *Chem. Phys.* **225**, 107 (1997).
- ⁵⁵R. G. Bray and M. J. Berry, *J. Chem. Phys.* **71**, 4909 (1979).
- ⁵⁶S. Shi and W. H. Miller, *Theor. Chim. Acta* **68**, 1 (1989).
- ⁵⁷K. V. Reddy, D. F. Heller, and M. J. Berry, *J. Chem. Phys.* **76**, 2814 (1982).
- ⁵⁸L. Halonen, *Chem. Phys. Lett.* **87**, 221 (1982).
- ⁵⁹R. H. Page, Y. R. Shen, and Y. T. Lee, *J. Chem. Phys.* **88**, 4621 (1988).
- ⁶⁰R. H. Page, Y. R. Shen, and Y. T. Lee, *J. Chem. Phys.* **88**, 5362 (1988).
- ⁶¹M. Scotoni, A. Boschetti, N. Oberhofer, and D. Bassi, *J. Chem. Phys.* **94**, 971 (1991).
- ⁶²F. Iachello and S. Oss, *J. Mol. Spectrosc.* **153**, 225 (1992).
- ⁶³J. A. Nicholson and W. D. Lawrance, *Chem. Phys. Lett.* **236**, 336 (1995).
- ⁶⁴A. Callegari, H. K. Srivastava, U. Merker, K. K. Lehmann, G. Scoles, and M. Davis, *J. Chem. Phys.* **106**, 432 (1997).
- ⁶⁵S. Rashev, M. Stamova, and S. Djambova, *J. Chem. Phys.* **108**, 4797 (1998).
- ⁶⁶P. Pulay, G. Fogarasi, and J. E. Boggs, *J. Chem. Phys.* **74**, 3999 (1981).
- ⁶⁷L. Goodman, A. G. Ozkabak, and S. N. Thakur, *J. Phys. Chem.* **95**, 9044 (1991).
- ⁶⁸C. J. O'Brien, "Improvement to an infrared laser-molecular beam spectrometer for IVR studies," Senior thesis, Princeton University, 1994.
- ⁶⁹J. E. Gambogi, M. Becucci, C. J. O'Brien, K. K. Lehmann, and G. Scoles, *Ber. Bunsenges. Phys. Chem.* **99**, 548 (1995).
- ⁷⁰K. Chen and E. S. Yeung, *J. Chem. Phys.* **69**, 43 (1978).
- ⁷¹G. Herzberg, *Molecular Spectra and Molecular Structure* (Van Nostrand, New York, 1945), Vol. II. Infrared and Raman spectra of polyatomic molecules.
- ⁷²D. Romanini and K. K. Lehmann, *J. Chem. Phys.* **98**, 6437 (1993).
- ⁷³B. Pate, K. Lehmann, and G. Scoles, *J. Chem. Phys.* **95**, 3891 (1991).
- ⁷⁴M. Quack, *J. Chem. Phys.* **82**, 3277 (1985).
- ⁷⁵W. Lawrence and A. Knight, *J. Phys. Chem.* **89**, 917 (1985).
- ⁷⁶E. J. Heller and R. L. Sundberg, in *Chaotic Behavior in Quantum Systems*, Vol. 120 of NATO ASI, edited by G. Casati (Plenum, Como, Italy, 1985), pp. 255–292.
- ⁷⁷F. J. Dyson and M. L. Mehta, *J. Math. Phys.* **4**, 701 (1963).
- ⁷⁸K. K. Lehmann and S. L. Coy, *J. Chem. Phys.* **87**, 5415 (1987).
- ⁷⁹P. E. Bevington and D. K. Robinson, *Data Reduction and Error Analysis for the Physical Sciences*, 2nd ed. (McGraw-Hill, New York, 1992).
- ⁸⁰S. Brandt, *Statistical and Computational Methods in Data Analysis* (North-Holland, Amsterdam, 1970).
- ⁸¹M. Robnik, *Prog. Theor. Phys. Suppl.* **116**, 331 (1994).
- ⁸²K. K. Lehmann and S. L. Coy, *Ber. Bunsenges. Phys. Chem.* **92**, 306 (1988).
- ⁸³T. Oka, *J. Chem. Phys.* **47**, 5410 (1967).
- ⁸⁴C. S. Parmenter, *Faraday Discuss. Chem. Soc.* **75**, 7 (1983).
- ⁸⁵D. Madsen, R. Pearman, and M. Gruebele, *J. Chem. Phys.* **106**, 5874 (1997).
- ⁸⁶R. Pearman and M. Gruebele, *J. Chem. Phys.* **108**, 6561 (1998).
- ⁸⁷M. Quack, in *Femtosecond Chemistry*, edited by J. Manz and L. Wöste (Verlag Chemie, Weinheim, 1994), pp. 781–818.
- ⁸⁸S. Mukamel, J. Sue, and A. Pandey, *Chem. Phys. Lett.* **105**, 134 (1984).

Erratum: "Intramolecular vibrational redistribution in aromatic molecules. I. Eigenstate resolved CH stretch first overtone spectra of benzene" [J. Chem. Phys. 113, 10583 (2000)]

A. Callegari,^{a)} U. Merker,^{b)} P. Engels,^{b),c)} H. K. Srivastava, K. K. Lehmann, and G. Scoles^{d)}

Department of Chemistry, Princeton University, Princeton, New Jersey 08544

[DOI: 10.1063/1.1347028]

Due to a production error, incorrect versions of Figs. 2 (p. 10586) and 7 (p. 10593) appeared in the original paper. AIP apologizes for this error. Corrected versions of Figs. 2 and 7 are reproduced below.

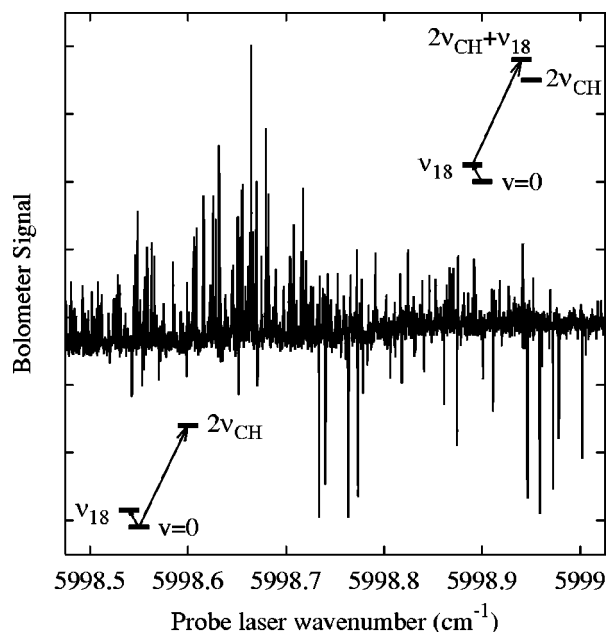


FIG. 2. The double resonance molecular beam spectrum of benzene observed with the probe laser tuned to the region of the CH stretch first overtone. Downward-going peaks correspond to transitions from the ground state, depleted by the pump laser, to the $\nu_{\text{CH}}=2$ pure overtone manifold. Upward-going peaks correspond to transitions from the upper state (ν_{18}) populated by the pump laser, to the $2\nu_{\text{CH}} + \nu_{18}$ manifold.

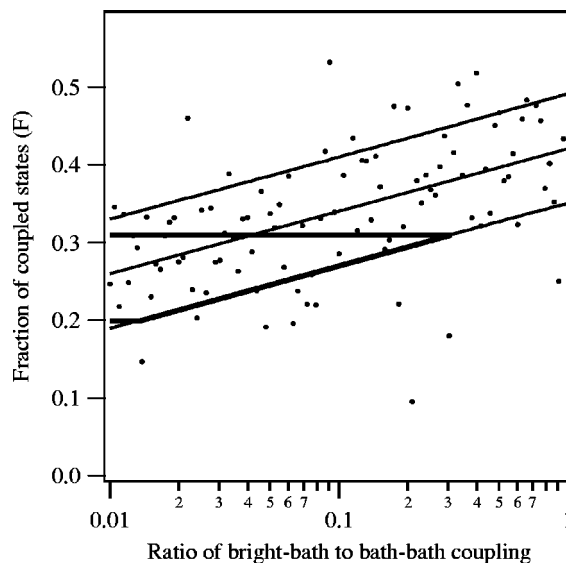


FIG. 7. The calculated fraction (F) of available states accessed by the IVR dynamics as a function of the bright state–bath to bath–bath coupling ratio. Thin lines show the result of a pseudolinear fit and the 1σ confidence bands. The thick lines show the region compatible with the range of values of F observed experimentally.

^{a)} Current address: Laboratoire de Chimie Physique Moléculaire (LCPM), École Polytechnique Fédérale de Lausanne, CH-1015 Lausanne, Switzerland.

^{b)} On leave from the University of Bonn, Institut für Angewandte Physik, Wegelerstr. 8, 53115 Bonn, Germany.

^{c)} Current address: Institut für Quantenoptik, Universität Hannover, Welfengarten 1, 30167 Hannover, Germany.

^{d)} Author to whom correspondence should be addressed. Electronic mail: gscoles@princeton.edu